

## **Supporting Information:**

# **Synthesis, Crystal Structures, Photophysical Properties and Bioimaging of Living Cells of Bis- $\beta$ -Diketonate Phenothiazine Ligands and its Cyclic Dinuclear Complexes**

*Dongmei Li,<sup>†</sup> Xiaohe Tian,<sup>‡</sup> Guiju Hu,<sup>†</sup> Qiong Zhang,<sup>†</sup> Peng Wang,<sup>†</sup> Pingping Sun,<sup>†</sup> Hongping Zhou,<sup>†</sup> Xiangming Meng,<sup>†</sup> Jiaxiang Yang,<sup>†</sup> Jieying Wu,<sup>†</sup> Baokang Jin,<sup>†</sup> Shengyi Zhang,<sup>†</sup> Xutang Tao,<sup>§</sup> Yupeng Tian,<sup>\*,†,‡,||</sup>*

<sup>†</sup>Department of Chemistry, Key Laboratory of Functional Inorganic Materials of Chemistry of Anhui Province, Anhui University, Hefei 230039, P.R. China; <sup>‡</sup>Department of Biomedical Science, University of Sheffield, Sheffield, UK; <sup>§</sup>State Key Laboratory of Crystal Materials, Shandong University, Jinan 250100, P.R. China; <sup>||</sup>State Key Laboratory of Coordination Chemistry, Nanjing University Nanjing 210093, P. R. China

<b>Part 1 Synthesis of the complexes</b> .....	S3
<b>1. Cd<sub>2</sub>Pv<sub>4</sub>L<sup>1</sup><sub>2</sub> (2).</b> .....	S3
<b>2. [Ni<sub>2</sub>Pv<sub>4</sub>L<sup>1</sup><sub>2</sub>]·3C<sub>6</sub>H<sub>6</sub> (3).</b> .....	S3
<b>3. Mn<sub>2</sub>Pv<sub>4</sub>L<sup>1</sup><sub>2</sub> (4).</b> .....	S3
<b>4. [Cu<sub>2</sub>L<sup>1</sup><sub>2</sub>]·2DMF (5).</b> .....	S3
<b>5. Co<sub>2</sub>Pv<sub>4</sub>L<sup>1</sup><sub>2</sub> (6).</b> .....	S3
<b>6. Cd<sub>2</sub>Pv<sub>4</sub>L<sup>2</sup><sub>2</sub> (8).</b> .....	S4
<b>7. Ni<sub>2</sub>Pv<sub>4</sub>L<sup>2</sup><sub>2</sub> (9).</b> .....	S4
<b>8. Mn<sub>2</sub>Pv<sub>4</sub>L<sup>2</sup><sub>2</sub> (10).</b> .....	S4
<b>9. [Cu<sub>2</sub>Pv<sub>2</sub>L<sup>2</sup><sub>2</sub>]·2C<sub>6</sub>H<sub>6</sub> (11).</b> .....	S4
<b>10. Co<sub>2</sub>Pv<sub>4</sub>L<sup>2</sup><sub>2</sub> (12).</b> .....	S5
<b>Part 2 Crystal Structure Determinations</b> .....	S5
<b>Figure S1.</b> (a) View showing the 1D column along the <i>a</i> -axis of complex 7. Inset: showing 1D channels. (b) 1D columns interacted with each other through edge-to-face $\pi$ - $\pi$ interactions to generate a 3D structure (Black balls represent the centroids of benzene rings). .....	S6
<b>Figure S2.</b> (a) The ORTEP structure of [Zn <sub>2</sub> Pv <sub>4</sub> L <sup>1</sup> <sub>2</sub> ]·2Py (1) (50% thermal ellipsoid probability). (b) View showing the 1D column along the <i>b</i> -axis. All hydrogen atoms are omitted for clarity. ....	S7
<b>Figure S3.</b> The ORTEP structure of 8 (50% thermal ellipsoid probability). All hydrogen atoms and solvents molecules are omitted for clarity. ....	S7
<b>Figure S4.</b> The ORTEP structure of 9 (50% thermal ellipsoid probability). All hydrogen atoms are omitted for clarity. ....	S7
<b>Figure S5.</b> The ORTEP structure of 10 (50% thermal ellipsoid probability). All hydrogen atoms are omitted for clarity. ....	S8

<b>Figure S6.</b> The ORTEP structure of <b>11</b> (50% thermal ellipsoid probability). All hydrogen atoms are omitted for clarity.	S8
<b>Figure S7.</b> The ORTEP structure of <b>12</b> (50% thermal ellipsoid probability). All hydrogen atoms are omitted for clarity.	S8
<b>Table S1.</b> Crystal data and structure refinement parameters for the compounds $\text{H}_2\text{L}^1$ , <b>1</b> , <b>7</b> and <b>8</b>	S9
<b>Table S2.</b> Crystal data and structure refinement parameters for <b>9-12</b> .	S9
<b>Table S3.</b> Selected bond lengths [Å] and angles [°] for $\text{H}_2\text{L}^1$ .	S10
<b>Table S4.</b> Selected bond lengths [Å] and angles [°] for complex <b>7</b> .	S10
<b>Table S5.</b> Selected bond lengths [Å] and angles [°] for complex <b>1</b> .	S11
<b>Table S6.</b> Selected bond lengths [Å] and angles [°] for complex <b>8</b> .	S11
<b>Part 3</b>	S12
<b>Figure S8.</b> Linear absorption (left) and OPEF (right) spectra of $\text{H}_2\text{L}^1$ in six solvents, $c = 10 \mu\text{M}$ .	S12
<b>Figure S9.</b> Linear absorption (left) and OPEF (right) spectra of $\text{H}_2\text{L}^2$ in six solvents, $c = 10 \mu\text{M}$ .	S12
<b>Figure S10.</b> Linear absorption (left) and OPEF (right) spectra of $\text{H}_2\text{L}^1$ in six solvents, $c = 1.0 \mu\text{M}$ .	S12
<b>Figure S11.</b> Spatial plots of the selected frontier molecular orbitals of the enol form of $(\text{L}^2)^{2-}$ . The time-dependent hybrid density functional theory (TDDFT) calculations were performed using B3LYP/6-31G*/6-31G**.	S13
<b>Figure S12.</b> Linear absorption (left) and OPEF (right) spectra of $\text{H}_2\text{L}^2$ , $(\text{L}^2)^{2-}$ and its complexes in THF, $c = 10 \mu\text{M}$ .	S13
<b>Table S7.</b> Photophysical data of all the compounds	S14
<b>Part 4</b>	S15
<b>Figure S13.</b> Log-Log linear of squared dependence of induced fluorescence signal and incident irradiance intensity of two ligands and complexes <b>1</b> , <b>2</b> , <b>7</b> and <b>8</b> .	S15
<b>Part 5</b>	S16
<b>Table S8.</b> Cell viability (%) of HeLa cells after incubation for 24 h with different concentration of the chromophores	S16
<b>Figure S14.</b> The variable temperature $^1\text{H}$ NMR of $\text{Zn}_2\text{Py}_2\text{L}^2$ .	S16
<b>Figure S15.</b> MALDI-TOF Mass spectrometry of <b>7</b>	S17
<b>References</b>	S17

## Part 1 Synthesis of the complexes

The synthetic route:  $M(OAc)_2 \cdot nH_2O$  (0.13 mmol) and bis- $\beta$ -diketones (0.06 mmol) were dissolved in 5 mL of pyridine. The solution was stirred at room temperature until a lot of precipitation formed and then filtered. The crude product was washed by dichloromethane (15 mL  $\times$  3) and then  $CH_3CN$  (15 mL  $\times$  3).

### 1. $Cd_2Py_4L_2$ (2).

Orange solid was obtained by above synthetic route, yield: 38 mg (80%).  $^1H$  NMR (400 MHz,  $d_6$ -DMSO)  $\delta$  (ppm): 1.35 (t,  $J$  = 6.5 and 6.5 Hz, 6H), 4.00 (q,  $J$  = 6.3, 6.0 and 6.3 Hz, 4H), 6.50 (s, 4H), 6.99 (d,  $J$  = 8.5 Hz, 4H), 7.41 (m, 20H), 7.72 (s, 4H), 7.79 (m, 8H), 7.93 (d,  $J$  = 6.5 Hz, 8H), 8.58 (s, 8H).  $^{13}C$  NMR (100 MHz,  $d_6$ -DMSO)  $\delta$  (ppm): 12.84, 42.13, 92.05, 115.02, 122.02, 124.43, 126.34, 127.06, 127.369, 128.56, 130.57, 136.72, 142.391, 145.50, 150.05, 184.10, 185.52. IR (KBr) ( $cm^{-1}$ ): 2983 and 2925 ( $\nu_{C-H}$ , aliphatic), 1588 ( $\nu_{C=O}$ , carbonyl), 758 and 700 ( $\gamma_{C-H}$ , pyridine). Anal. calcd for  $C_{84}H_{66}Cd_2N_6O_8S_2$ : C, 64.00; H, 4.22; N, 5.33; O, 8.12; S, 4.07 %. Found: C, 64.08; H, 4.13; N, 5.24; O, 8.31; S, 4.15 %. TGA analysis: the first weight loss occurred at 180 °C corresponding to the loss of four coordinated pyridine units (20.0 %). The main structure decomposed at 371 °C.

### 2. $[Ni_2Py_4L_2] \cdot 3C_6H_6$ (3).

### 3. $Mn_2Py_4L_2$ (4).

Orange solid was obtained by above synthetic route, yield: 38 mg (80 %). IR (KBr) ( $cm^{-1}$ ): 2983 and 2925 ( $\nu_{C-H}$ , aliphatic), 1593 ( $\nu_{C=O}$ , carbonyl), 762 and 797 ( $\gamma_{C-H}$ , pyridine). Anal. Calcd. for  $C_{84}H_{66}Mn_2N_6O_8S_2$ : C, 69.03; H, 4.55; N, 5.75; O, 8.76; S, 4.39 %. Found: C, 68.97; H, 4.62; N, 5.81; O, 8.82; S, 4.45%. TGA analysis: the first weight loss occurred at 190 °C corresponding to the loss of four coordinated pyridine units (21.6 %). The main structure decomposed at 410 °C.

### 4. $[Cu_2L_2] \cdot 2DMF$ (5).

### 5. $Co_2Py_4L_2$ (6).

Orange solid was obtained by above synthetic route, yield: 40 mg (91 %). IR (KBr) ( $cm^{-1}$ ): 2976 and 2926 ( $\nu_{C-H}$ , aliphatic), 1591 ( $\nu_{C=O}$ , carbonyl), 758 and 699 ( $\gamma_{C-H}$ , pyridine). Anal. Calcd. for  $C_{84}H_{66}Co_2N_6O_8S_2$ : C, 68.66; H, 4.53; N, 5.72; O, 8.71; S, 4.36%. Found: C, 68.57; H, 4.59; N, 5.80; O, 8.65; S, 4.42%. TGA analysis: the first weight loss occurred at 180 °C corresponding to the loss of four coordinated pyridine units (21.8 %). The main structure decomposed at 410 °C.

## **6. Cd<sub>2</sub>Py<sub>4</sub>L<sup>2</sup> (8).**

H<sub>2</sub>L<sup>2</sup> (0.20 mmol, 0.10 g) in 5 mL of pyridine was added into a 50 mL colorimetric tube, layered with 15 mL benzene, and then a solution of Cd(OAc)<sub>2</sub>·H<sub>2</sub>O (0.40 mmol, 0.2 mg) in pyridine (5 mL). Orange single crystals for X-ray analysis were obtained on the walls of the *vial* in a few days, yield: 56 mg (35 %). Anal. calcd for C<sub>64</sub>H<sub>46</sub>Cd<sub>2</sub>F<sub>12</sub>N<sub>6</sub>O<sub>8</sub>S<sub>2</sub>: C, 49.78; H, 3.00; N, 5.44; O, 8.29; S, 4.15 %. Found: C, 49.67; H, 3.03; N, 5.56; O, 8.20; S, 4.07 %. IR (KBr) (cm<sup>-1</sup>): 2981 and 2933 ( $\nu_{C-H}$ , aliphatic), 1620 ( $\nu_{C=O}$ , carbonyl), 1131 ( $\nu_{C-F}$ , trifluoromethyl), 785 ( $\chi_{C-H}$ , aromatic), 751 and 700 ( $\chi_{C-H}$ , pyridine). <sup>1</sup>H NMR (400 MHz, d<sub>6</sub>-DMSO) δ (ppm): 1.31 (t, 6H), 3.98 (q, 4H), 6.81 (s, 4H), 7.07 (d, 4H), 7.39 (m, 8H), 7.53 (m, 4H), 7.79 (t, 4H), 7.93 (s, 4H), 8.58 (d, 8H). <sup>13</sup>C NMR (100 MHz, d<sub>6</sub>-DMSO) δ (ppm): 12.70, 42.32, 89.68, 115.45, 122.09, 124.41, 126.25, 127.83, 134.21, 136.70, 146.45, 150.07, 162.77, 178.22. TGA analysis: the first weight loss occurred at 180 °C corresponding to the loss of four coordinated pyridine units (20.4 %). The main structure decomposed at 390 °C.

## **7. Ni<sub>2</sub>Py<sub>4</sub>L<sup>2</sup> (9).**

Above crude product again dissolved in THF/acetonitrile (v/v 3/1), orange, plate crystals were obtained, yield: 20 mg (47 %). IR (KBr) (cm<sup>-1</sup>): 2979 and 2923 ( $\nu_{C-H}$ , aliphatic), 1618 ( $\nu_{C=O}$ , carbonyl), 1137 ( $\nu_{C-F}$ , trifluoromethyl), 758 and 698 ( $\chi_{C-H}$ , pyridine). Anal. Calcd. for C<sub>64</sub>H<sub>46</sub>F<sub>12</sub>N<sub>6</sub>Ni<sub>2</sub>O<sub>8</sub>S<sub>2</sub>: C, 53.51; H, 3.23; N, 5.85; O, 8.91; S, 4.46%. Found: C, 53.46; H, 3.19; N, 5.94; O, 8.96; S, 4.39%. TGA analysis: the first major weight loss occurred at 180 °C corresponding to the loss of coordinated pyridine units (21.9 %). The main structure decomposed at 426 °C.

## **8. Mn<sub>2</sub>Py<sub>4</sub>L<sup>2</sup> (10).**

Orange, plate crystals were obtained through the same way as that of **9**, yield: 25 mg (58 %). IR (KBr) (cm<sup>-1</sup>): 2982 and 2933 ( $\nu_{C-H}$ , aliphatic), 1613 ( $\nu_{C=O}$ , carbonyl), 1132 ( $\nu_{C-F}$ , trifluoromethyl), 753 and 700 ( $\chi_{C-H}$ , pyridine). Anal. Calcd. for C<sub>64</sub>H<sub>46</sub>F<sub>12</sub>Mn<sub>2</sub>N<sub>6</sub>O<sub>8</sub>S<sub>2</sub>: C, 53.79; H, 3.24; N, 5.88; O, 8.96; S, 4.49%. Found: C, 53.67; H, 3.35; N, 5.79; O, 9.02; S, 4.40%. TGA analysis: the first major weight loss occurred at 190 °C corresponding to the loss of coordinated pyridine units (22.1 %). The main structure decomposed at 380 °C.

## **9. [Cu<sub>2</sub>Py<sub>2</sub>L<sup>2</sup>]<sup>2+</sup>·2C<sub>6</sub>H<sub>6</sub> (11).**

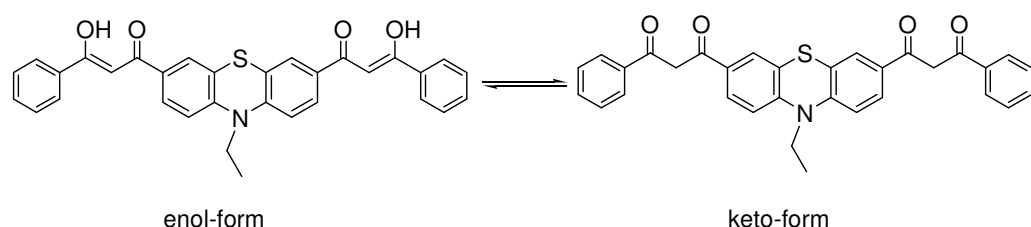
H<sub>2</sub>L<sup>2</sup> (0.06 mmol) in 5 mL of pyridine was added into a 50 mL colorimetric tube, layered with 15 mL benzene, and then a solution of Cu(OAc)<sub>2</sub>·H<sub>2</sub>O (0.13 mmol) in pyridine (5 mL). Red crystals were obtained on the walls of the *vial* in a few days, yield: 33 mg (77 %). IR (KBr) (cm<sup>-1</sup>): 2981 and 2932 ( $\nu_{C-H}$ , aliphatic), 1613 ( $\nu_{C=O}$ , carbonyl), 1132 ( $\nu_{C-F}$ , trifluoromethyl), 758 ( $\chi_{C-H}$ , pyridine). Anal. Calcd. for C<sub>66</sub>H<sub>48</sub>Cu<sub>2</sub>F<sub>12</sub>N<sub>4</sub>O<sub>8</sub>S<sub>2</sub>: C, 54.88; H, 3.35; N, 3.88; O, 8.86; S, 4.44%. Found: C, 54.76; H, 3.28; N,

3.69; O, 8.77; S, 4.32%. TGA analysis: the first stage of weight loss occurred at 105 °C corresponding to the loss of two solvent benzene molecules (10.8 %). The second stage at 210 °C was corresponding to the loss of coordinated pyridine units (10.9 %). The main structure decomposed at 461 °C.

### 10. $\text{Co}_2\text{Py}_4\text{L}^2_2$ (12).

Orange, plate crystals were obtained through the same way as that of **9**, yield: 18 mg (42 %). IR (KBr) ( $\text{cm}^{-1}$ ): 2982 and 2931 ( $\nu_{\text{C}-\text{H}}$ , aliphatic), 1621 ( $\nu_{\text{C}=\text{O}}$ , carbonyl), 1136 ( $\nu_{\text{C}-\text{F}}$ , trifluoromethyl), 755 and 701 ( $\gamma_{\text{C}-\text{H}}$ , pyridine). Anal. Calcd. for  $\text{C}_{64}\text{H}_{46}\text{Co}_2\text{F}_{12}\text{N}_6\text{O}_8\text{S}_2$ : C, 53.49; H, 3.23; N, 5.85; O, 8.91; S, 4.46%. Found: C, 53.38; H, 3.31; N, 5.80; O, 8.85; S, 4.41%. TGA analysis: the first weight loss occurred at 220 °C corresponding to the loss of coordinated pyridine molecules (21.9 %). The main structure decomposed at 415 °C.

**Scheme S1.** The keto-enol tautomerisation of  $\text{H}_2\text{L}^1$ .

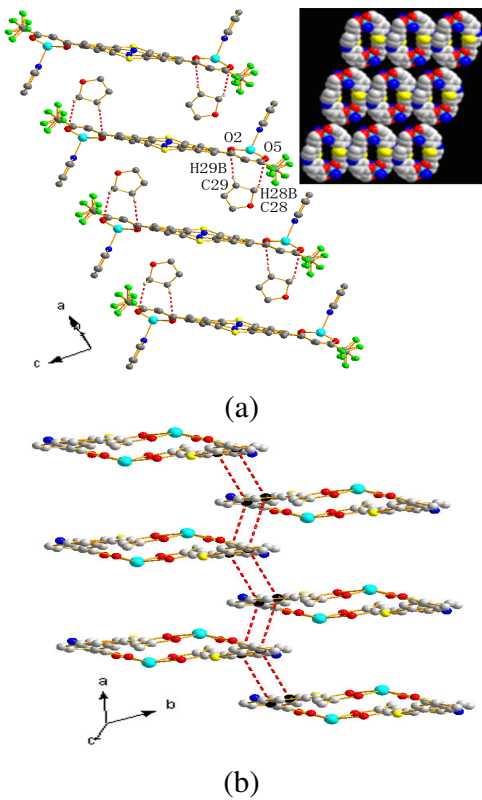


## Part 2 Crystal Structure Determinations

The molecular structures of **7**, **1**, **8**, **9**, **10**, **11** and **12** were shown in Figures S1-S7. The unit cell, data collection and refinement parameters are located in the following Tables S1-S2. Table S3-S6 show selected bond lengths and angles of  $\text{H}_2\text{L}^1$ , **1**, **7**, **8**.

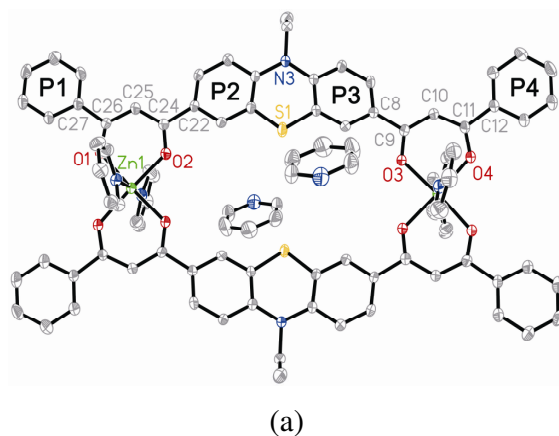
**Type I – four coordination.** The structure of this type appears only in  $[\text{Cu}_2\text{L}^1_2]\cdot 2\text{DMF}$  (**5**). **5** crystallizes in the monoclinic space group  $P2_1/c$ . Each Cu(II) center has a square planar coordinated sphere surrounded by four oxygen atoms from two  $\beta$ -diketonato fragments. This kind of structure has been described by us before.<sup>1</sup>

**Type II – five coordination.** In Figure S1a, an infinite 1D columnar arrangement along  $a$ -axis has been found, which was stabilized by the hydrogen bonding interactions formed between O atoms of the ligand and H(C) atoms of solvent THF molecule [ $d(\text{O}2\cdots\text{H}29\text{B}(\text{C}29)) = 2.710 \text{ \AA}$ ,  $d(\text{O}2\cdots\text{C}29) = 3.596 \text{ \AA}$ ,  $\angle(\text{C}29-\text{H}29\text{B}\cdots\text{O}2) = 152.08^\circ$ ;  $[d(\text{O}5\cdots\text{H}28\text{B}(\text{C}28)) = 2.716 \text{ \AA}$ ,  $d(\text{O}5\cdots\text{C}28) = 3.348 \text{ \AA}$ ,  $\angle(\text{C}28-\text{H}28\text{B}\cdots\text{O}5) = 123.23^\circ]$ . The 1D structure also incorporates 1D channels down  $a$ -axis (Figure S1a, inset). 1D columns are linked each other through edge-to-face  $\pi\cdots\pi$  stacking interactions to form a 3D framework [the centroid-centroid separation is  $4.553 \text{ \AA}$ ; the ring planes intersect at an angle of  $11.36^\circ$ ]<sup>2</sup> (Figure S1b).



**Figure S1.** (a) View showing the 1D column along the *a*-axis of complex **7**. Inset: showing 1D channels. (b) 1D columns interacted with each other through edge-to-face  $\pi$ - $\pi$  interactions to generate a 3D structure (Black balls represent the centroids of benzene rings).

**Type III – six coordination.** Different from **3**, complex molecules of **1** interact with each other through H-bondings formed between O atoms of the ligand and H(C) atoms of the pyridine rings to form 1D columns down *b*-axis [ $d(O3 \cdots H35(C35)) = 2.670 \text{ \AA}$ ,  $d(O3 \cdots C35) = 3.285 \text{ \AA}$ ,  $\angle(C35-H35 \cdots O3) = 124.35^\circ$ ] (Figure S2b). The 1D structure also incorporates 1D channels down *b*-axis. As the same as that of **7**, 1D columns linked to each other through edge-to-face  $\pi$ - $\pi$  stacking interactions to be a 3D framework [the centroid–centroid separations is  $4.279 \text{ \AA}$ ; the ring planes intersect at an angle of  $21.40^\circ$ ].



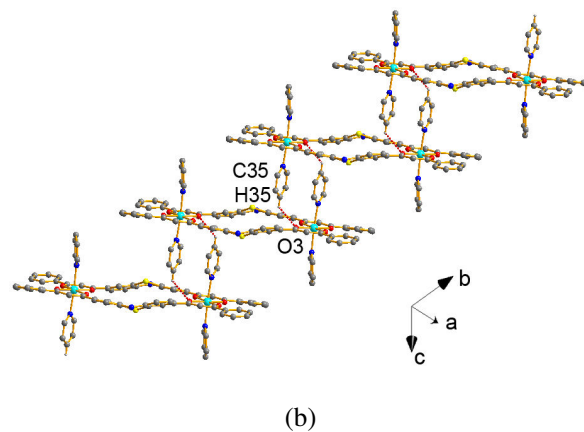


**Figure S2.** (a) The ORTEP structure of  $[\text{Zn}_2\text{Py}_4\text{L}^1_2]\cdot 2\text{Py}$  (**1**) (50% thermal ellipsoid probability). (b) View showing the 1D column along the *b*-axis. All hydrogen atoms are omitted for clarity.

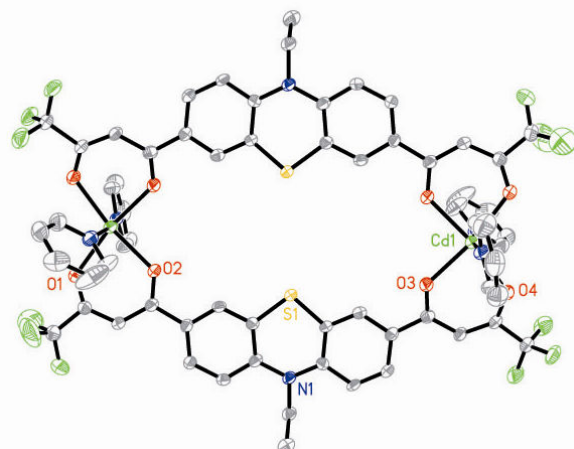


**Figure S3.** The ORTEP structure of **8** (50% thermal ellipsoid probability). All hydrogen atoms and solvents molecules are omitted for clarity.

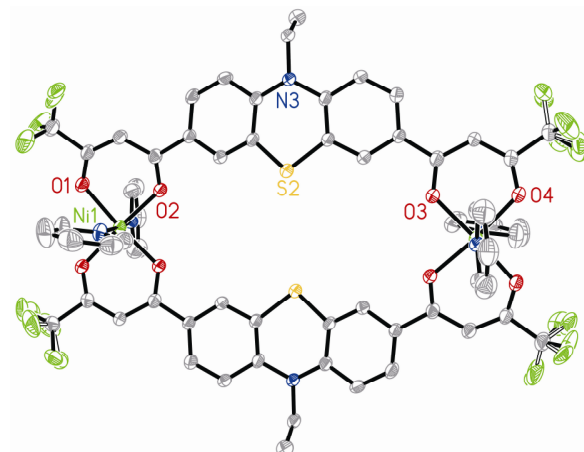


**Figure S4.** The ORTEP structure of **9** (50% thermal ellipsoid probability). All hydrogen atoms are omitted for clarity.

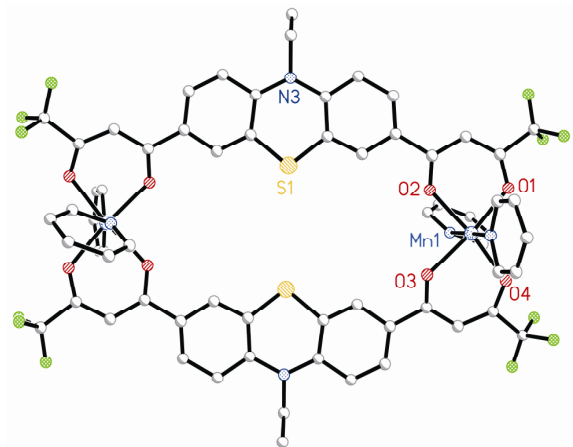


**Figure S5.** The ORTEP structure of **10** (50% thermal ellipsoid probability). All hydrogen atoms are omitted for clarity.

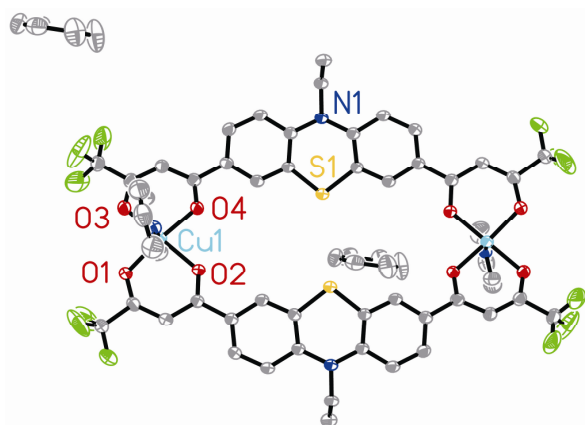


**Figure S6.** The ORTEP structure of **11** (50% thermal ellipsoid probability). All hydrogen atoms are omitted for clarity.

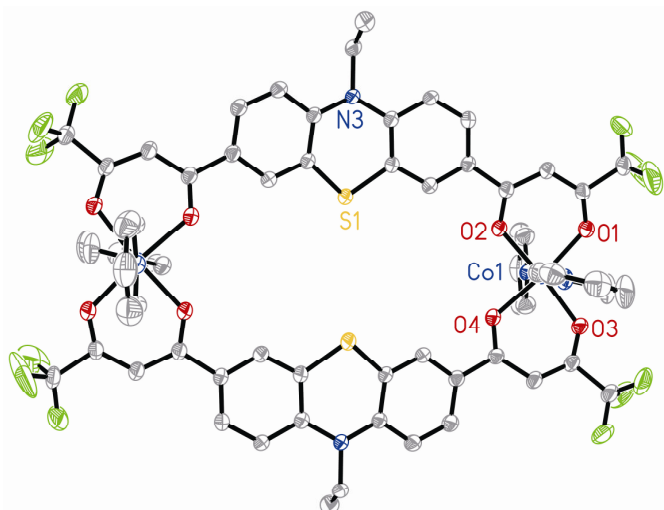


**Figure S7.** The ORTEP structure of **12** (50% thermal ellipsoid probability). All hydrogen atoms are omitted for clarity.

**Table S1.** Crystal data and structure refinement parameters for the compounds **H<sub>2</sub>L<sup>1</sup>**, **1**, **7** and **8**.

	<b>H<sub>2</sub>L<sup>1</sup></b>	<b>1</b>	<b>7</b>	<b>8</b>
CCDC	298940	660612	673738	711281
formula	C <sub>32</sub> H <sub>25</sub> NO <sub>4</sub> S	C <sub>94</sub> H <sub>76</sub> N <sub>8</sub> O <sub>8</sub> S <sub>2</sub> Zn <sub>2</sub>	C <sub>62</sub> H <sub>52</sub> F <sub>12</sub> N <sub>4</sub> O <sub>10</sub> S <sub>2</sub> Zn <sub>2</sub>	C <sub>64</sub> H <sub>46</sub> Cd <sub>2</sub> F <sub>12</sub> N <sub>6</sub> O <sub>8</sub> S <sub>2</sub>
fw	519.59	1636.38	1435.94	1543.99
cryst system	Monoclinic	Triclinic	Triclinic	Triclinic
Space group	P2 <sub>1</sub> /c	P $\bar{1}$	P $\bar{1}$	P $\bar{1}$
a/ $\text{\AA}$	15.276(5)	11.092(5)	8.925(7)	8.896(5)
b/ $\text{\AA}$	16.211(5)	12.371(5)	9.851(7)	10.216(5)
c/ $\text{\AA}$	10.466(3)	15.530(5)	19.046(13)	18.837(5)
$\alpha^{\circ}$		100.918(5)	88.040(11)	92.476(5)
$\beta^{\circ}$	98.021(4)	105.277(5)	83.163(12)	99.680(5)
$\gamma^{\circ}$		95.784(5)	64.338(9)	113.835(5)
V/ $\text{\AA}^3$	2566.4(13)	936.8(7)	1498.3(19)	1531.9(12)
Z	4	2	1	2
D <sub>c</sub> /g cm <sup>-3</sup>	1.345	1.103	1.585	2.910
F(000)	1088	684	728	1235
T/K	293(2)	293(2)	293(2)	298(2)
$\lambda/\text{\AA}$	0.71073	0.71073	0.71073	0.71073
$\theta_{\min-\max}/^{\circ}$	1.84, 25.10	2.36, 21.10	2.15, 25.05	1.10, 25.00
N <sub>ref</sub> , N <sub>par</sub>	4485, 343	7789, 515	5239, 416	5367, 425
R [I>2 $\sigma$ (I)]	0.0487	0.0577	0.0766	0.0579
R (all data)	0.1096	0.1410	0.1662	0.0841
GOF on F <sup>2</sup>	1.022	0.925	0.999	1.087

**Table S2.** Crystal data and structure refinement parameters for **9-12**.

	<b>9</b>	<b>10</b>	<b>11</b>	<b>12</b>
CCDC	660613	673759	700927	700930
formula	C <sub>64</sub> H <sub>46</sub> Ni <sub>2</sub> F <sub>12</sub> N <sub>6</sub> O <sub>8</sub> S <sub>2</sub>	C <sub>64</sub> H <sub>46</sub> Mn <sub>2</sub> F <sub>12</sub> N <sub>6</sub> O <sub>8</sub> S <sub>2</sub>	C <sub>66</sub> H <sub>48</sub> Cu <sub>2</sub> F <sub>12</sub> N <sub>4</sub> O <sub>8</sub> S <sub>2</sub>	C <sub>64</sub> H <sub>46</sub> Co <sub>2</sub> F <sub>12</sub> N <sub>6</sub> O <sub>8</sub> S <sub>2</sub>
fw	1436.58	1429.07	1444.28	1437.05
cryst Syst	Triclinic	Triclinic	Triclinic	Triclinic
Space group	P $\bar{1}$	P $\bar{1}$	P $\bar{1}$	P $\bar{1}$
a / $\text{\AA}$	8.675(5)	8.544(6)	9.3769(2)	8.7278(14)
b / $\text{\AA}$	9.988(5)	9.937(7)	9.9380(2)	10.0793(15)
c / $\text{\AA}$	19.371(5)	19.474(13)	19.0906(4)	19.420(3)
$\alpha/{}^{\circ}$	89.890(5)	91.086(8)	86.1590(10)	89.497(11)
$\beta/{}^{\circ}$	83.436(5)	96.614(9)	82.3120(10)	83.290(11)
$\gamma/{}^{\circ}$	66.425(5)	111.179(8)	63.4480(10)	66.211(11)
V / $\text{\AA}^3$	1526.5(12)	1528.2(17)	1577.02(6)	1551.2(4)
Z	2	2	1	1
D <sub>c</sub> / g cm <sup>-3</sup>	1.391	1.553	1.521	1.538
F(000)	648	726	734	730
T (K)	298(2)	298(2)	296(2)	296(2)
$\lambda/\text{\AA}$	0.71069	0.71073	0.71073	0.71073
$\theta_{\min-\max}/{}^{\circ}$	2.12,26.06	2.11,25.00	2.29, 24.74	2.41,24.99
N <sub>ref</sub> , N <sub>par</sub>	5979,483	5231,368	7213,425	7108, 425
R (I>2 $\sigma$ (I))	0.048	0.1472	0.0543	0.0569
R (all data)	0.0877	0.1822	0.0726	0.1065
GOF	1.097	0.996	1.037	1.039

**Table S3.** Selected bond lengths [ $\text{\AA}$ ] and angles [ $^\circ$ ] for  $\mathbf{H}_2\mathbf{L}^1$ .

Bond	lengths	Bond	angles
C5–C7	1.470(5)	O1–C7–C8	121.2(4)
C7–O1	1.289(5)	C8–C7–C5	121.7(4)
C7–C8	1.403(5)	C9–C8–C7	119.8(4)
C8–C9	1.393(6)	O2–C9–C8	120.8(4)
C9–O2	1.276(5)	O2–C9–C10	117.3(4)
C9–C10	1.504(4)	C8–C9–C10	121.9(4)
C22–O3	1.281(4)	O3–C22–C23	120.1(4)
C22–C23	1.410(5)	O3–C22–C19	117.2(3)
C22–C19	1.498(4)	C23–C22–C19	122.7(3)
C23–C24	1.379(5)	C24–C23–C22	120.8(4)
C24–O4	1.304(4)	O4–C24–C23	120.7(4)
C24–C25	1.476(4)	C23–C24–C25	124.3(3)

**Table S4.** Selected bond lengths [ $\text{\AA}$ ] and angles [ $^\circ$ ] for complex **7**.

Bond	lengths	Bond	angles
O2–Zn1	2.001(4)	O5–C2–C3	129.0(7)
O3–Zn1	1.989(5)	C3–C2–C1	117.7(7)
O4–Zn1	1.990(5)	C2–C3–C4	124.9(6)
O5–Zn1	2.004(5)	O2–C4–C3	123.1(6)
C1–C2	1.498(11)	C3–C4–C5	121.1(6)
C2–O5	1.245(7)	O3–C19–C20	121.7(6)
C2–C3	1.335(9)	C20–C19–C18	120.5(6)
C3–C4	1.379(9)	C21–C20–C19	123.9(6)
C4–O2	1.241(7)	O4–C21–C20	130.9(7)
C4–C5	1.471(8)	C20–C21–C22	117.2(7)
C18–C19	1.460(9)	O3–Zn1–O4	87.9(2)
C19–O3	1.247(7)	O3–Zn1–O2	84.15(19)
C19–C20	1.405(9)	O2–Zn1–O5	87.77(19)
C20–C21	1.320(9)	O3–Zn1–O5	158.6(2)
C21–O4	1.242(7)	O4–Zn1–O5	91.0(2)

**Table S5.** Selected bond lengths [Å] and angles [°] for complex **1**.

Bond	lengths	Bond	angles
Zn1–O2	2.047(2)	O2–Zn1–O3	88.91(10)
Zn1–O3	2.060(3)	O2–Zn1–O1	87.05(10)
Zn1–O1	2.066(3)	O3–Zn1–O4	87.36(10)
Zn1–O4	2.069(2)	O1–Zn1–O4	96.74(10)
O3–C9	1.271(4)	C9–O3–Zn1	128.3(2)
O4–C11	1.274(4)	C11–O4–Zn1	128.3(2)
O1–C26	1.274(4)	C26–O1–Zn1	128.2(2)
O2–C24	1.264(4)	C26–C25–C24	124.7(4)
C8–C9	1.502(5)	C9–C10–C11	126.0(4)
C10–C9	1.400(5)	O1–C26–C25	125.5(4)
C10–C11	1.404(5)	C25–C26–C27	119.6(3)
C12–C11	1.500(5)	C9–O3–Zn1	128.3(2)
C22–C24	1.507(5)	C24–O2–Zn1	129.3(2)
C25–C26	1.405(5)	O4–C11–C10	124.7(3)
C25–C24	1.410(5)	C10–C11–C12	119.4(4)
C27–C26	1.510(5)	C10–C9–C8	119.5(3)

**Table S6.** Selected bond lengths [Å] and angles [°] for complex **8**.

Bond	lengths	Bond	angles
Cd1–O1	2.221(5)	O1–Cd1–O3	170.06(16)
Cd1–O2	2.273(4)	O1–Cd1–O4	108.29(17)
Cd1–O3	2.234(4)	O3–Cd1–O4	81.64(16)
Cd1–O4	2.257(5)	O1–Cd1–O2	81.51(17)
Cd1–N2	2.380(6)	O3–Cd1–O2	88.55(16)
Cd1–N3	2.291(6)	O4–Cd1–O2	169.25(16)
C2–C1	1.479(3)	O1–Cd1–N3	89.61(19)
C3–C2	1.380(9)	O3–Cd1–N3	90.94(19)
C3–C4	1.393(9)	O4–Cd1–N3	89.75(18)
C5–C4	1.491(9)	O2–Cd1–N3	94.83(18)
O1–C2	1.245(8)	O1–Cd1–N(2)	82.51(19)
O2–C4	1.264(7)	O3–Cd1–N2	98.21(19)
O3–C17	1.252(7)	O4–Cd1–N2	85.16(18)
O4–C19	1.247(7)	O2–Cd1–N2	91.93(19)
C16–C17	1.459(9)	N3–Cd1–N2	168.76(19)
C18–C17	1.425(9)	C2–C3–C4	126.9(6)
C18–C19	1.352(9)	C19–C18–C17	127.4(6)

### Part 3

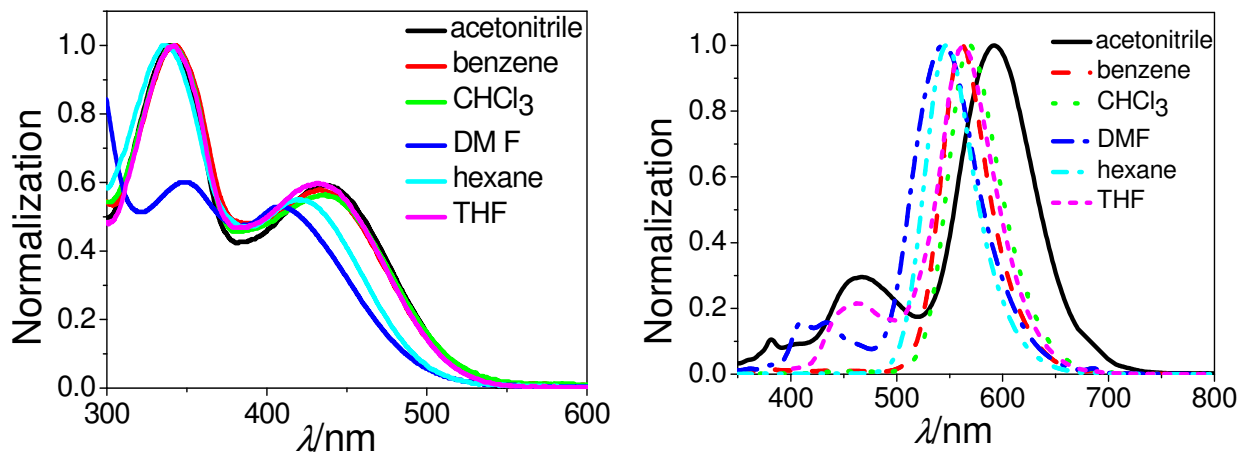


**Figure S8.** Linear absorption (left) and OPEF (right) spectra of  $\mathbf{H}_2\mathbf{L}^1$  in six solvents,  $c = 10 \mu\text{M}$ .

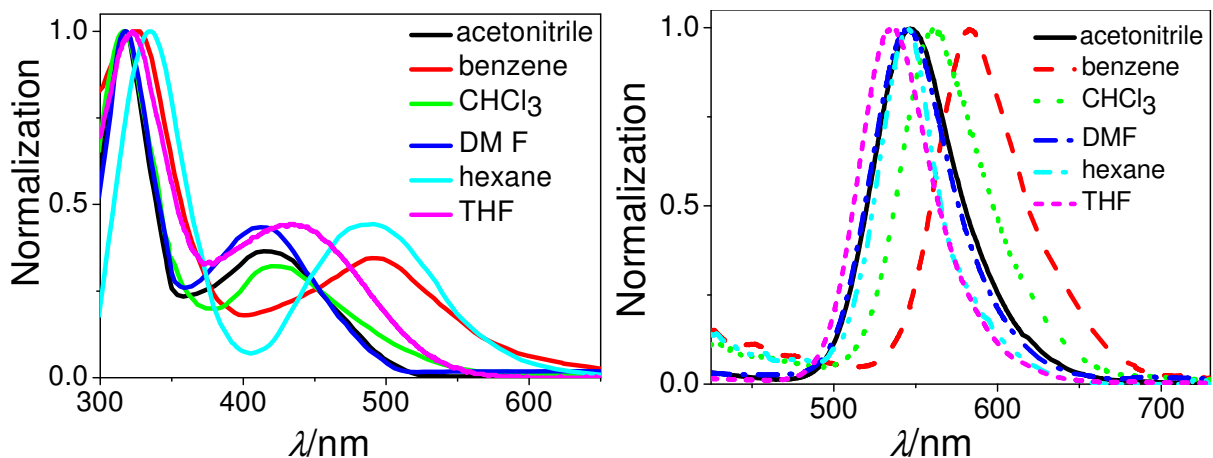


**Figure S9.** Linear absorption (left) and OPEF (right) spectra of  $\mathbf{H}_2\mathbf{L}^2$  in six solvents,  $c = 10 \mu\text{M}$ .

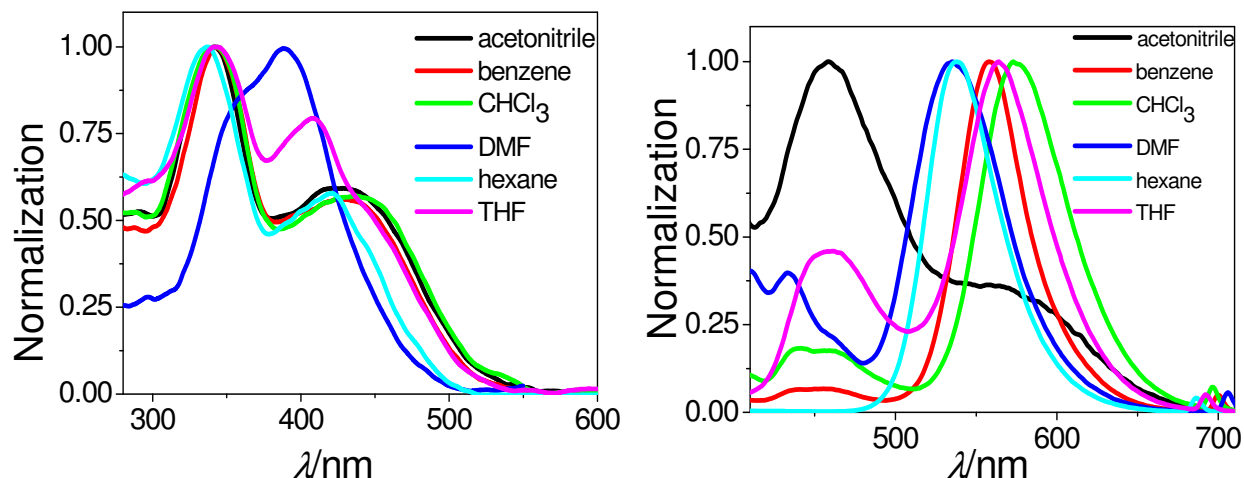


**Figure S10.** Linear absorption (left) and OPEF (right) spectra of  $\mathbf{H}_2\mathbf{L}^1$  in six solvents,  $c = 1.0 \mu\text{M}$ .

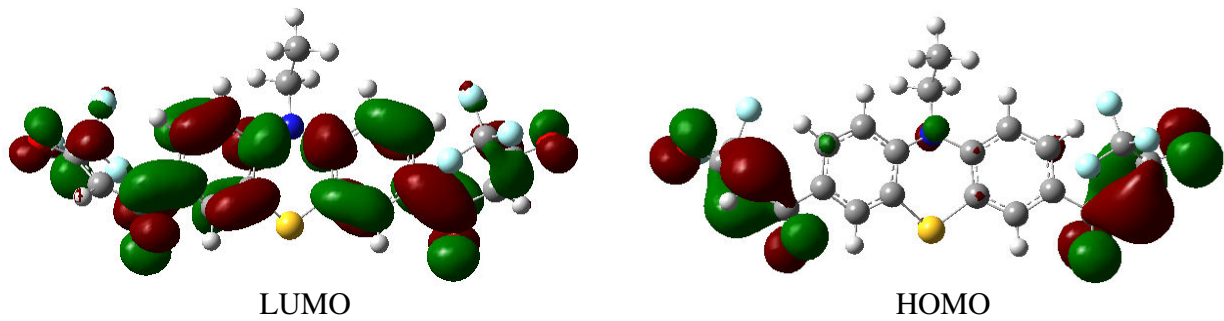


**Figure S11.** Spatial plots of the selected frontier molecular orbitals of the enol form of  $(\text{L}^2)^{2-}$ . The time-dependent hybrid density functional theory (TDDFT) calculations were performed using B3LYP /6-31G\*//6-31G\*\*.

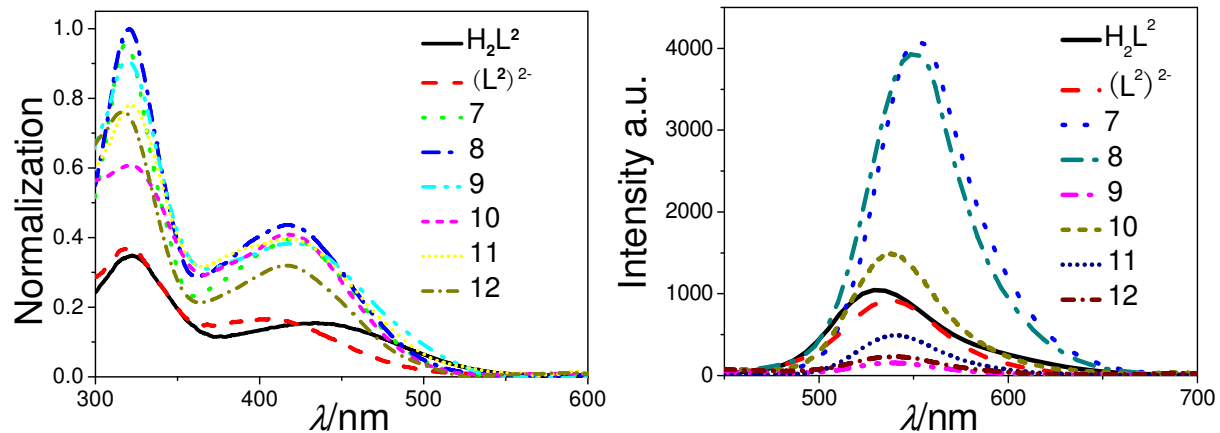


**Figure S12.** Linear absorption (left) and OPEF (right) spectra of  $\text{H}_2\text{L}^2$ ,  $(\text{L}^2)^{2-}$  and its complexes in THF,  $c = 10 \mu\text{M}$ .

**Table S7.** Photophysical data of all the compounds.

Compd	Solvent	$\lambda_{ab}$ (nm)	$\varepsilon (\times 10^4 \text{ dm}^3 \text{ mol}^{-1} \text{ cm}^{-1})$	$\lambda_{em}$ (nm)	${}^a\lambda_{em}^{\text{TP}}$	${}^b\phi$	${}^c\tau$	${}^d\delta_{\max}$
<b>H<sub>2</sub>L<sup>1</sup></b>	Hexane	335, 419		529				
	Benzene	342, 434		556				
	CHCl <sub>3</sub>	339, 434		572				
	THF	341, 433	3.6, 2.1	465, 563	570	0.38	6.29	155
	CH <sub>3</sub> CN	338, 438		457, 565				
	DMF	350, 415		534				
	solid			621				
<sup>e</sup> Cal.	enol	336, 446			499	0.71		790
	keto	402			677	0.22		6031
(L <sup>1</sup> ) <sup>2</sup>	THF	342, 428	3.8, 2.3	561	508	0.35	7.05	21
<b>1</b>	THF	342, 412	6.8, 5.6	544	541	0.32	5.83	568
<b>2</b>	THF	344, 418	6.9, 4.5	562	538	0.27	6.20	664
<b>3</b>	THF	342, 422	6.0, 4.4	543				
<b>4</b>	THF	345, 425	5.9, 4.2	543				
<b>5</b>	THF	341, 431	4.8, 3.5	544				
<b>6</b>	THF	341, 428	8.0, 6.8	545				
<b>H<sub>2</sub>L<sup>2</sup></b>	Hexane	334, 491		543				
	Benzene	325, 492		582				
	CHCl <sub>3</sub>	316, 423		560				
	THF	322, 434	2.6, 1.1	536	547	0.46	7.03	204
	CH <sub>3</sub> CN	318, 420		547				
	DMF	317, 414		545				
	solid			632				
Cal.	enol	338, 462			528	0.36		812
(L <sup>2</sup> ) <sup>2</sup>	THF	319, 402	2.8, 1.2	538	598	0.51	4.32	28
<b>7</b>	THF	318, 419	7.0, 2.9	553	560	0.32	7.37	369
<b>8</b>	THF	320, 417	7.4, 3.2	550	557	0.30	7.45	366
<b>9</b>	THF	320, 419	6.7, 2.8	537				
<b>10</b>	THF	321, 417	4.5, 3.0	537				
<b>11</b>	THF	321, 417	5.8, 2.9	538				
<b>12</b>	THF	317, 416	5.6, 2.4	535				

<sup>a</sup> Peak position of TPEF in nm. <sup>b</sup> The fluorescence quantum yield. <sup>c</sup> Fluorescence lifetime in ns. <sup>d</sup> TPA cross-section in GM. <sup>e</sup> Calculated results.

## Part 4

The emission intensity of  $\mathbf{H}_2\mathbf{L}^1$ ,  $\mathbf{H}_2\mathbf{L}^2$ , **1**, **2**, **7** and **8** investigated at 780 nm were shown in Figure S13. The linear dependence on the square of input laser power suggests that it is obviously a two-photon excitation mechanism.

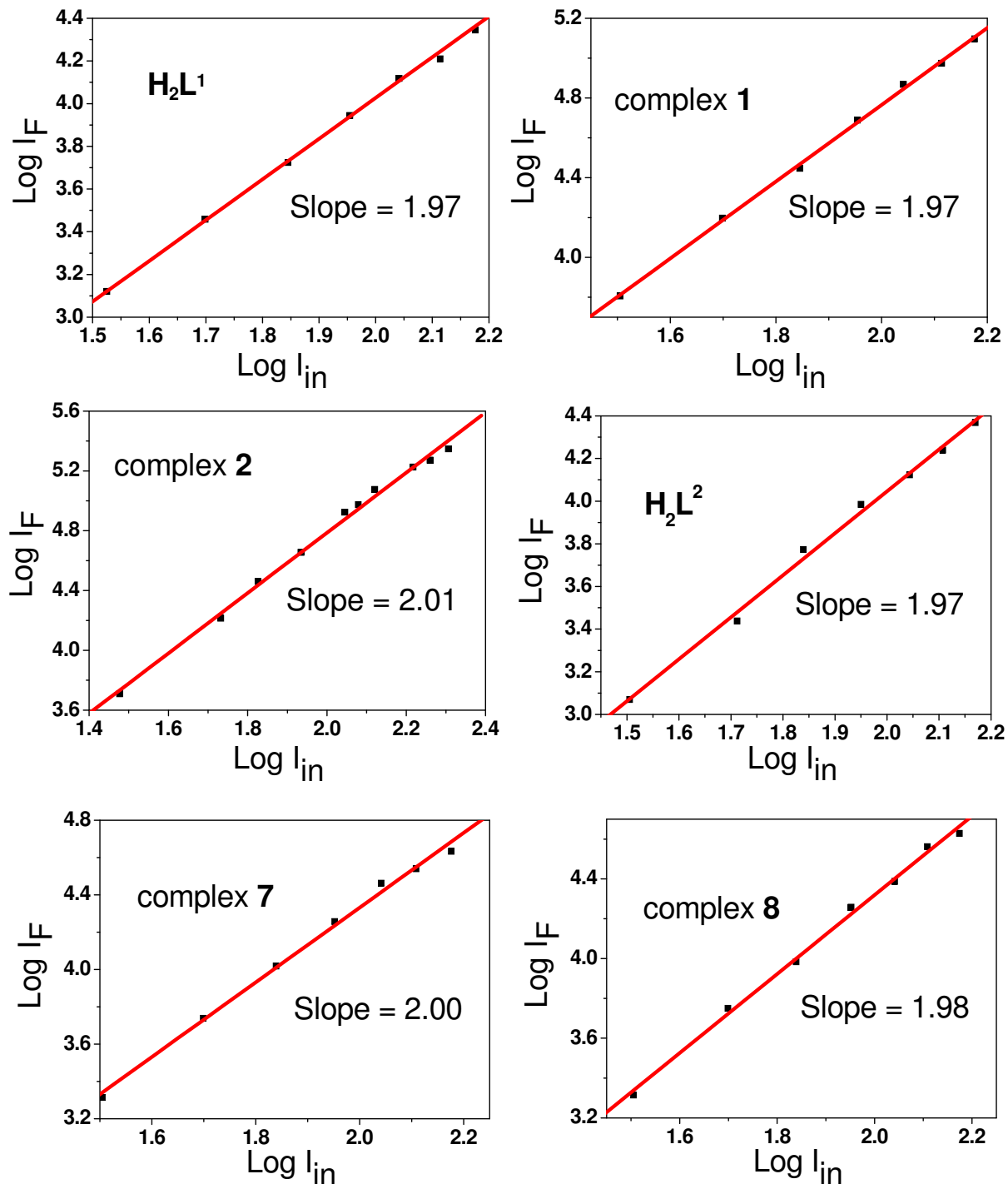


**Figure S13.** Log–Log linear of squared dependence of induced fluorescence signal and incident irradiance intensity of two ligands and complexes **1**, **2**, **7** and **8**.

## Part 5

**Table S8.** Cell viability (%) of HeLa cells after incubation for 24 h with different concentration of the chromophores.

Compd./viability(%)	Concentration ( $\mu\text{M}$ )	10	20	50	100
<b>H<sub>2</sub>L<sup>1</sup></b>		99.46 $\pm$ 5.95	95.57 $\pm$ 3.48	79.18 $\pm$ 3.46	65.11 $\pm$ 2.06
<b>H<sub>2</sub>L<sup>2</sup></b>		97.50 $\pm$ 1.78	91.58 $\pm$ 3.49	78.24 $\pm$ 2.66	55.38 $\pm$ 5.33
<b>1</b>		95.16 $\pm$ 3.25	87.62 $\pm$ 2.65	75.81 $\pm$ 3.17	64.42 $\pm$ 5.7
<b>7</b>		96.49 $\pm$ 3.23	90.20 $\pm$ 3.99	75.43 $\pm$ 2.79	58 $\pm$ 2.03

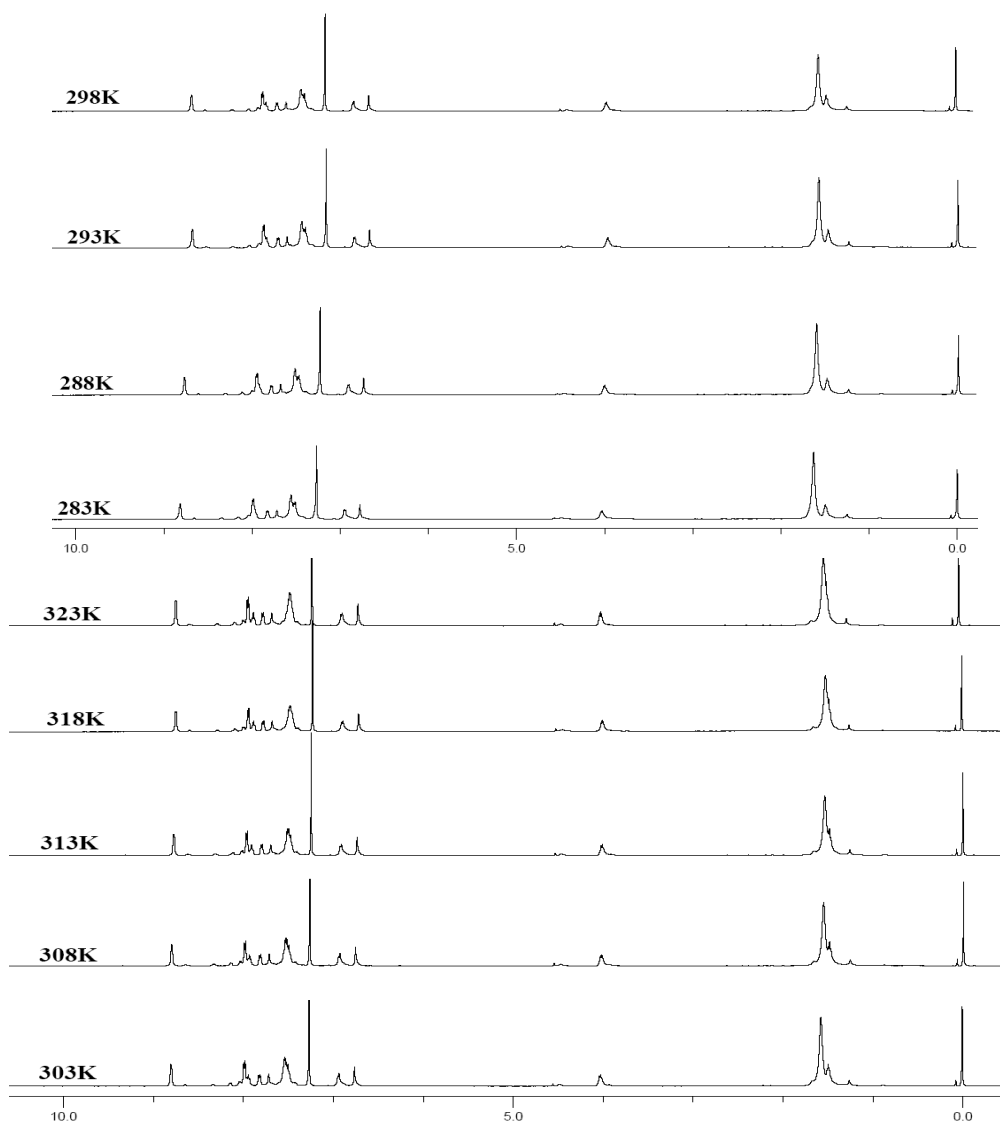


**Figure S14** The variable temperature <sup>1</sup>H NMR of  $\text{Zn}_2\text{Py}_2\text{L}^2$

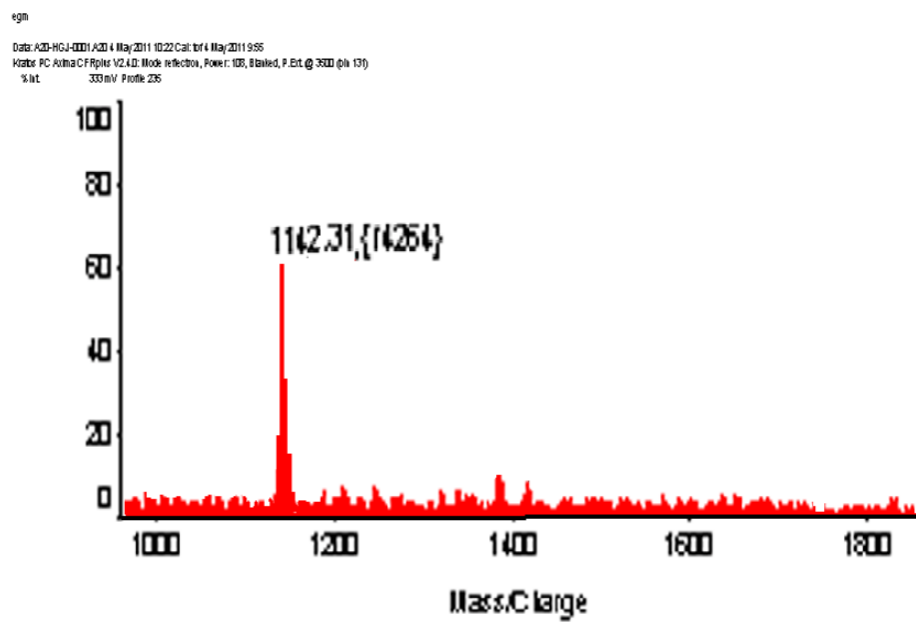


**Figure S15** MALDI-TOF Mass spectrometry of **7**

## References

- (1) Li, D. M.; Zhou, W.; Xu, G. Y.; Zhou, H. P.; Wu, J. Y.; Tian, Y. P.; Tao, X. T.; Jiang, M. H. *J. Mol. Struct.* **2009**, 929, 120.
- (2) Quan, R. W.; Li, Z.; Jacobsen, E. N. *J. Am. Chem. Soc.* **1996**, 118, 8156.